

Performance Analysis of Hybrid Controller in Smib System Using Metaheuristic Optimization Techniques Under Different Design Criteria

¹NIDHI SAHU, ²MAHESH SINGH, ³SHIMPY RALHAN

1,2,3 Department of Electrical and Electronics Engineering,
Shri Shankaracharya technical campus, SSGI, Bhilai (C.G), INDIA

Abstract: Regardless of the dynamic behavior, structures may also be seen in an integrated manner, rather than as an individual way. This paper assesses the reliability development of the SMIB. The MATLAB is used to analyze the system's reaction as a Simulink method. The synchronous unit, excitation mechanism and FOPID-PSS are the three most critical components for study of the SMIB system. Most control units configured to decrease the noise at low frequencies. Here robust controller is used to enhance stability and reduce machine vibrations. For incorporate the reliability criterion, an optimization strategy is used. The high rate of convergence over the optimization of the ant colony and the harmony search algorithm favors the eagle perching optimization.

KeyWords: Ant Colony Optimization (ACO), Harmony Search (HS) Algorithm, Eagle Perching Optimization (EPO), FOPID-PSS, Design Criteria, Single Machine Infinite Bus (SMIB) system.

1 Introduction

Generation, transmission and distribution are three primary aspects under which power system reliability plays a significant part [1]. Factors may have a major effect on device actions, such as: rise in device voltage, usage of fast-speed excitation method, reduction in system transmission performance, reduction in generator input speed, errors and sudden variations in load. Instability raises the fluctuations in the device behaviour by raising the level of oscillations. The primary objective of the design and installation of the FOPID-PSS controller [2] is to regulate the characteristics of the controller and also to optimize system performance during failures and system disruptions. Various methods and control systems are used to enhance sensitivity, but PID-PSS provides the highest and most effective efficiency for the SMIB framework [3]. The FOPID-PSS, created by optimization techniques is

used because of its rigorous efficiency. It is challenging to set the FOPID-PSS values, so the optimization method can be used to set the variables, thereby preserving consistency.

ACO was first introduced by Dorigo and Gambardella. It's one of the multi-objective methods. This method is mainly focused on the actions of food-seeking ants [4]. The Ants normally stay in a group. At first, the ant crosses spontaneously in pursuit of food. As the ants get food, they revert back to the colony leaving their footprints named "pheromones" [5]. This footprint recognizes the food pathway. Instead they pick the shortest route to consume food. This technique of optimization has a poor convergence rate.

The Harmony search mechanism is a meta-heuristic algorithm that ultimately offers a sufficiently superior response for the targeted function to be modelled [6]. This technique was first developed by Joong Hoon Kim and Zong Woo

Geem. This method is basically influenced by a musical system. Although we want an ideal state and harmony in music, this method of optimization seeks harmony in the optimization system in the same way. Through preserving an outstanding state of unity, everybody finds happiness in song. Harmony search algorithm is a quick iterative method since its convergence rate is higher than that of ACO.

Eagle is a name that is often used for many large birds of prey belonging to a family of Accipitridae. They are usually 30 to 31 centimetres long with a wingspan of 6 to 7 feet. They usually stay in the air, even if there is time to reproduce male and female conduct a very blandishment ritual. They fly at high altitude. There they attach their clays together and collapse down while performing aerobics movements and shatter apart just before they touch the ground. Matron usually lays 2 to 4 eggs, their life cycle consists mainly of five cycles: incubating, nestling, adolescent phase and puberty. An eagle represents a class of predators. They feed mainly on fish, other marine species and small animals [7]. Their trapping is unique, they fly high towards possible height and from there they target their prey. Once followed, they dive for prey and catch that.

2 SMIB Model Representation

The linearized model of the synchronous machine experiences fluctuating behaviour, which is categorized as temporary behaviour and stationary behaviour. Figure 1 illustrates an SMIB system [8]. This paper is about checking for changes in the stable status of the network. The simple third-order system is sufficient for evaluating a single machine system.

$$\Delta E'_q = \frac{K_3}{1+K_3\tau'_{d0}s} \Delta E_{FD} - \frac{K_3K_4}{1+K_3\tau'_{d0}s} \Delta\delta \quad (1)$$

Were; E_{FD} = RMS value of E'_q , τ'_{d0} = transient time constant of direct-axis.

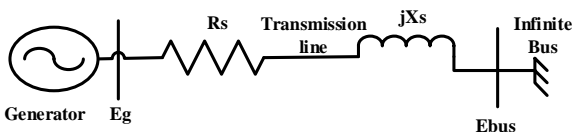


Fig1.Synchronous machine connected to infinite bus

Incremental electrical torque can be written as:

$$\Delta T_e = K_1\Delta\delta + K_2\Delta E'_q \quad (2)$$

Were; $\Delta\delta$ = change in torque angle, E'_q = stator voltage

$$E'_q = E + (x_d - x'_d)I_d \quad (3)$$

Were; E = RMS value of stator air gap voltage, I_d = Direct axis current

The synchronous generator terminal ΔV_t is written as:

$$\Delta V_t = K_5\Delta\delta + K_6\Delta E'_q \quad (4)$$

Were, ΔV_t is the linearized terminal voltage of synchronous generator.

NOTE: Gains constants K_1, K_2, K_3, K_4, K_5 and K_6 are contingent on the machine parameters. Generally K_1, K_2, K_3, K_4 and K_6 are positive whereas K_5 is positive for light and normal loading conditions and negative for heavy loading condition [1][8].

2.1 Model Representation of Excitation System

The primary function of the excitation device is to deliver current to the rotating segment of the machine, i.e. the winding of the rotor. Essentially, the excitation device is used to produce flux through feeding current to the field rotor winding of the synchronous device. This changes the voltage on the terminal field current by maintaining the terminal voltage steady, making it easier to hold the generator in sync. The excitation mechanism often plays a key function in increasing the efficiency of the network. Figure 2 demonstrates the method of excitation [9].

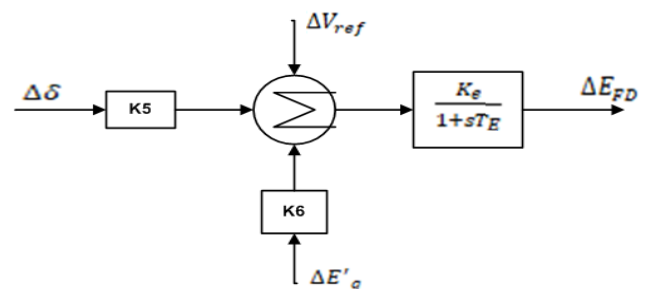


Fig.2. Representation of Excitation system

3 Explanation of FOPID-PSS

To boost the robustness and efficiency of PID controller, Podlubny has suggested an expansion to the PID control system which can be named as a fractional order PID (FOPID) controller due to the involvement of differentiator of order μ and integrator of order λ . The idea of the fractional differentiation integral is widely used in the Riemann-Liouville (RL) description [10]. The RL representation for the FOPID is written as:

$$\alpha D_t^\alpha F(t) = \frac{1}{\Gamma(n-\alpha)} \left(\frac{d}{dt}\right)^n \int_a^t \frac{f(\tau)}{(t-\tau)^{1-(n-\alpha)}} d\tau \quad (5)$$

Γ is the Euler's gamma function specifying the factorial significance and allocating the operator to obtain fractional order values. A replacement specification, predicated on the concept of fractional differentiation, as defined in Grunwald-Letnikov, is shown by:

$$\alpha D_t^\alpha F(t) = \lim_{g \rightarrow 0} \frac{1}{\Gamma(n-\alpha)} \sum_{d=0}^{(t-\alpha/g)} \frac{\Gamma(\alpha+d)}{\Gamma(g+1)} f(t-dg) \quad (6)$$

For FOPID transfer function is written as;

$$G(s) = K_p + K_i s^{-\lambda} + K_d s^\mu \quad (7)$$

3.1 FOPID-PSS model

PSS is a linear monitoring system attached to a synchronous machine for minimal-frequency quiet disturbances. Control system is often linked in parallel to the excitation system. The excitation system regulates the sensitive current with the help of AVR. PSS sends an extra control pulse to the AVR such that the synchronicity is retained. FOPID-PSS including voltage regulator is a very effective way to increase reliability in a steady state and reliability at voltage peaks. Here, one-stage PSS along with FOPID is used to boost reliability as it can produce better outcomes compared to two-stage PSS. The PSS is synchronized with the PID controller in order to increase reliability. FOPID-PSS involves stabilizer strengthening block, wash-out block and phase adjustment block [9]. The above listed blocks help mitigate PSS overreaction and damp device disturbances at the time of disturbance [10]. The coefficients defined by K_{pss} , T_1 , T_2 , P , I , D , μ and λ are built to provide damping during vibration.

Table 1 displays the spectrum of FOPID-PSS parameters [11].

FOPID control system design includes the following variables; P , I , D , μ and λ . Control system is highly versatile and allows the dynamic and complex characteristics of robust and flexible control system to be tuned. A new versatile hybrid stabilizer based on the traditional PSS and PID controller is proposed in this research to develop the optimized PSS (FOPID-PSS), by giving additional power system damping [10][11]. The device's transfer function to regulate the voltage of excitation is given by;

$$V_{PSS}(s) = \left[K_{pss} \left(\frac{sT_w}{1+sT_w} \right) \left(\frac{1+sT_1}{1+sT_2} \right) \right] [K_p + K_i s^{-\lambda} + K_d s^\mu] \Delta\omega(s) \quad (8)$$

Where; K_{pss} = washout gain of the stabilizer, T_w = washout time constant.

Figure 3 shows the single-stage PSS [2]. Above controller model includes a wash-out block and a lead lag block together known as phase compensation block which are used here to reduce the low frequency vibrations of the system during an intense performance. The PID-PSS parameters T_1 , T_2 , P , I and D are set, so that the vibrations are properly damped over the respective frequency range [1-4].

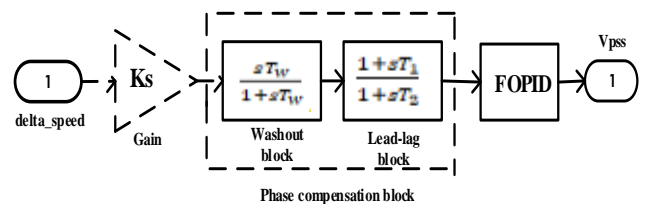


Fig.3. Representation of PID-Power System Stabilizer

$$V_{PSS}(s) = \left[K_{pss} \left(\frac{sT_w}{1+sT_w} \right) \left(\frac{1+sT_1}{1+sT_2} \right) \right] [K_p + K_i s^{-\lambda} + K_d s^\mu] \Delta\omega(s) \quad (9)$$

Below represents the range of FOPID-PSS parameters for performing optimization criteria. There are total eight parameters in FOPID-PSS design. K_{pss} , P , I , D , T_1 , T_2 , λ and μ are the eight parameters of fractional order PID-PSS controller.

Table1: Range of parameters for FOPID- PSS design

| Parameters of FOPID-PSS | Kpss | P | I | D | λ | μ | T1 | T2 |
|-------------------------|------|----|----|----|-----------|-------|----|----|
| Minimum bound | 0 | 0 | 0 | 0 | 0.1 | 0.1 | 0 | 0 |
| Maximum bound | 100 | 10 | 10 | 10 | 1 | 1 | 10 | 10 |

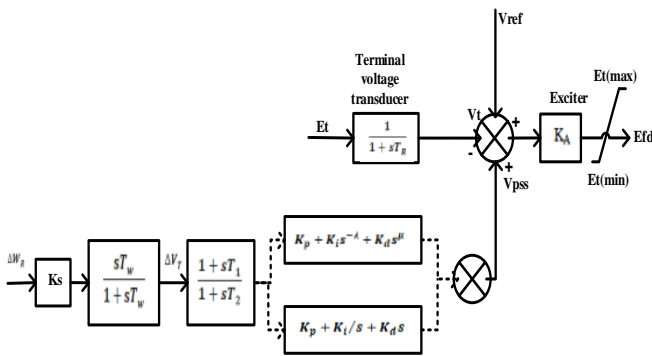


Fig 4. FOPID-PSS equipped excitation system

Figure 4 describes about the excitation system which is connected with FOPID-PSS and terminal voltage transducer. Input block consists of power system stabilizer and fractional order proportional integral derivative controller. Below section describes about the design of FOPID-PSS controller using eagle perching optimization technique.

4 FOPID-PSS design

4.1 Designing of FOPID-PSS parameters by applying Eagle Perching Optimization

Eagle Perching Optimization is a metaheuristic process which imparts progressive search. Since the rate of convergence of Eagle Perching Optimization is very fast as compared to ACO and HS, therefore it is used here to boost the performance of SMIB system [3]. EPO algorithm imitates the perching behaviour of eagle. Inspired by this behaviour this algorithm also searches the highest point of the solution. Maxima and minima function is the unique nature that defines working algorithm for all of its inhabitants and is represented as: $min(f) = max(-f)$ [7]. Key for performing reliable and stochastic optimization algorithm is the transformation of this algorithm from exploration to exploitation. Mathematical

representation of this algorithm is shown below:

$$I_{scale} = I_{scale} * eta \tag{10}$$

Where; I_{scale} = scaling variable, eta = shrinking constant

“eta” can be represented as; $(\frac{res}{I_{scale}})^{\frac{1}{ts}}$ where ts = maximum number of iterations.

Table 2: Eagle Perching Optimization Parameters implemented for the design of controller

| S.No | Optimization parameters for Eagle perching optimization | values |
|------|---|--------|
| i | Resolution Range (<i>res</i>) | 0.05 |
| ii | Shrinking Coefficient (<i>eta</i>) | 0.82 |
| iii | Area to search (<i>I_{scale}</i>) | 1000 |
| iv | No: of particles do search | 30 |
| v | No: of dimensions | 8 |
| vi | No: of iterations | 50 |

Above table represents the optimization parameters for implementing Eagle Perching Optimization. Optimization algorithm runs according to the above mentioned values. For obtaining best and desired solution values are set.

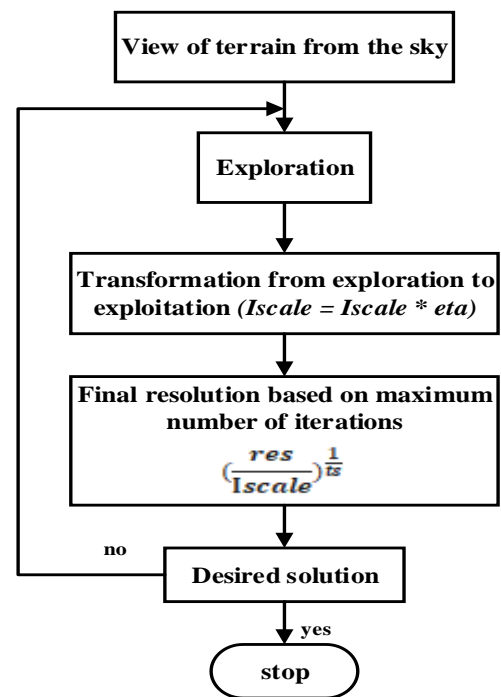


Fig5. Flow chart for Eagle Perching Optimization

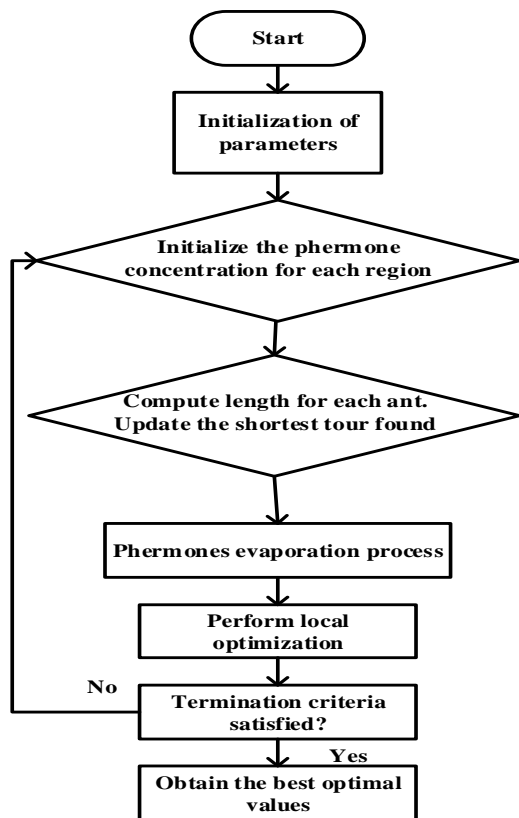


Fig6. Flow chart for Ant Colony Optimization

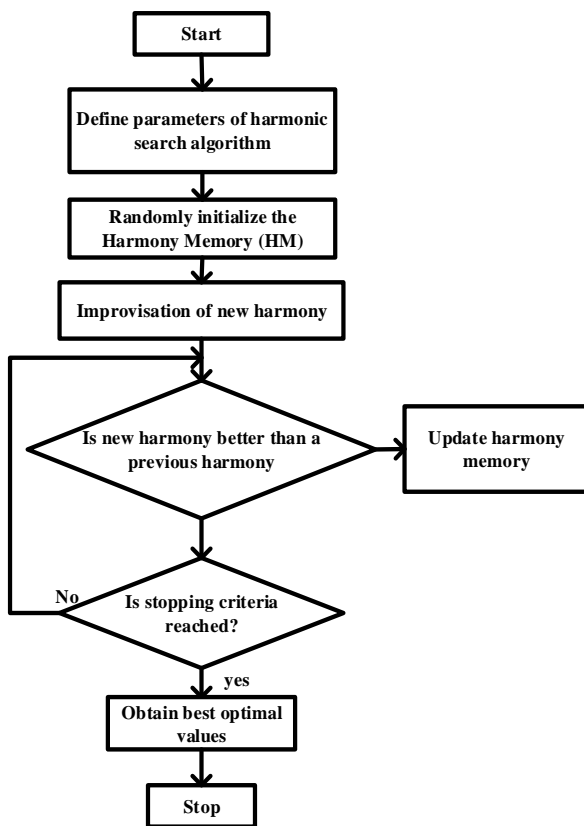


Fig7. Flow chart for Harmony Search Algorithm

Figure 5, 6 and 7 shows the flow chart for ACO [5], HS [6] and EPO [7] algorithm respectively. Step by step process, till desired solution obtained is represented in the flow chart. If the desired solution is not obtained then again algorithm continues till the desired solution is obtained [7]. This whole process is repeated till the optimal and desired solution is obtained. EPO gives best and desired solution to the problem.

5 Overall Representation of System

The system shown below is simulated in MATLAB / Simulink.

Figure 5 shows the block representation of system. It consists of three parts: synchronous machine, excitation system and controller block. All blocks are interlinked together to form overall system for obtaining optimal solution

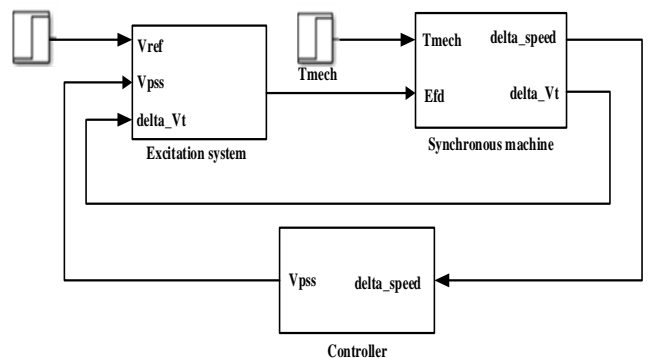


Fig8. Overall representation of Blocks

Below figures identifies individual representation of overall block representation. All sections were synchronized for stability efficiency. Figure 9 represents synchronous machine Heffron-Phillips model, [5] comprises primarily of a flux degrading coil and a torque angle coil. The layout should be implemented in MATLAB / Simulink. Figure 10 shows excitation mechanism and is defined by equations (3) and (4). Figure 11 represents controller block which consists of PID-PSS. The equation for controller is seen in equation (9). The PID-PSS displayed is based on the phase correction methodology. The speed variance is the input indicator for the controller and the Vpss is the output indicator for the controller which provides an extra stabilizing signal to the excitation mechanism [8].

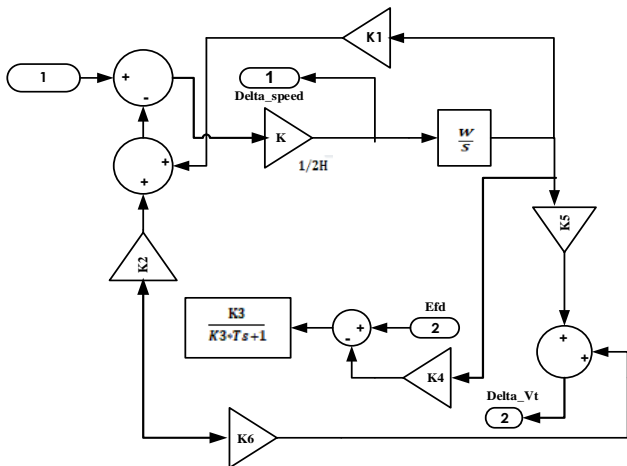


Fig9. Synchronous Machine

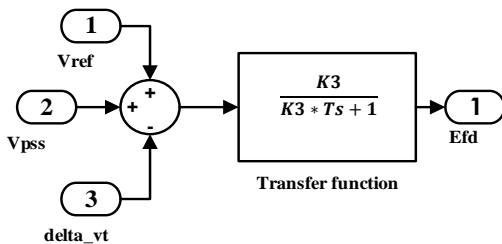


Fig10. Excitation System

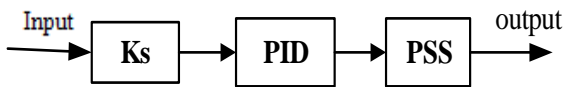


Fig11. Controller

6 Criteria Specification

Many design criteria is available depending on the suitability of the system. In this paper for ensuring the stability of the system three criteria's are used. Some of them are mentioned below [12-14].

- ITAE criteria
- ISE criteria
- IAE criteria

Above mentioned criteria are described below:

6.1 ITAE criteria

It stands for Integral time weighted absolute error. This parameter tests a decreased flaw in the method, resulting in a program that has a strong under-damped method [12]. The performance index in mathematical terms is shown by:

$$ITAE = \int_0^{\infty} t|e(t)|dt$$

Where; 't' is time, and e(t) is time difference to be regulated between point of operation and variable.

6.2. ISE criteria

It specifies square error integral of the system. This criterion penalizes machine errors that arise positively and negatively [13]. The performance index in mathematical terms is shown by:

$$ISE = \int_0^{\infty} e^2(t)dt$$

6.3. IAE criteria

It denotes absolute error integral [13] [14]. The performance index is represented by:

$$IAE = \int_0^{\infty} |e(t)|dt$$

Result analysis is done considering above three design criteria and the values are concluded. Below section gives detailed analysis of cases for SMIB system.

Below section describes about the different loading conditions according to which single machine infinite bus system operates. Respective active and reactive power for different cases is mentioned.

7 Analysis of cases

The efficiency of the SMIB is determined in the specified operational and working environments. Tests for various loading environments are measured and contrasted. Frequency variance, Variance of the terminal voltage is analyzed depending on the system's reaction [3].

Table 3: Operational status of single machine bus network

| Operational condition → | P1 | P2 | P3 |
|-------------------------|-----|-----|-----|
| Loading conditions ↓ | | | |
| Active Power(P) (Pu) | 1.8 | 1.5 | 0.7 |
| Reactive Power(Q) (Pu) | 1.0 | 0.8 | 0.3 |

Table 3 displays the various operating environments and working situations in which the system is worked as defined by P1 (full load), P2 (regular load) as P3 (luminous load) [8] [9].

8 Analysis of results

Result analysis is done on the basis of three design criteria, namely ITAE, IAE and ISE under different loading conditions.

8.1 Analysis on the basis of ITAE criteria

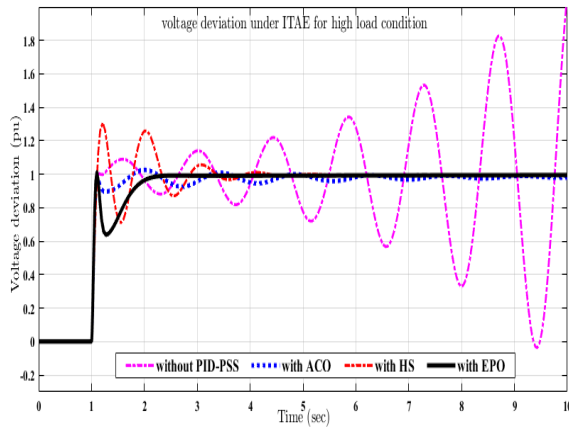


Fig 12 (a) Voltage deviation for full load condition

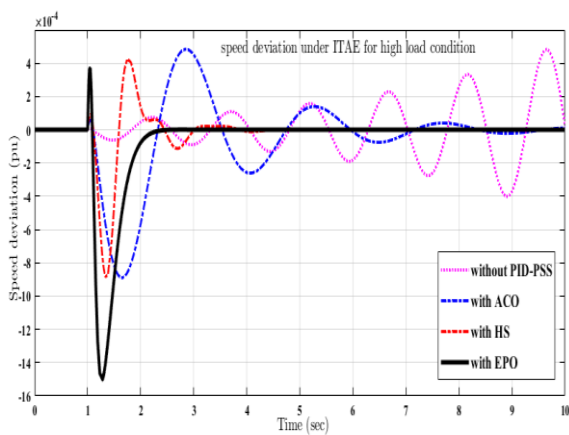


Fig 12 (b) Speed deviation for full load condition

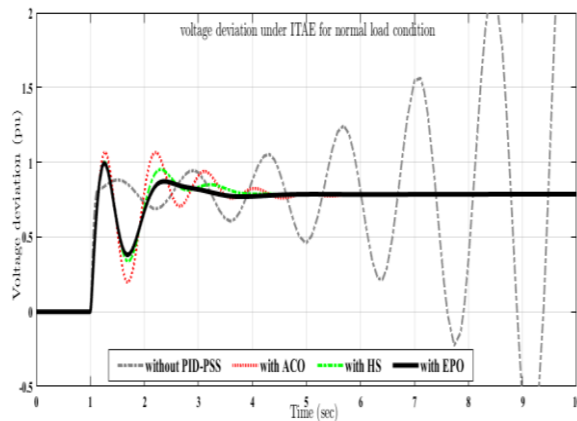


Fig 13 (a) Voltage deviation for regular load

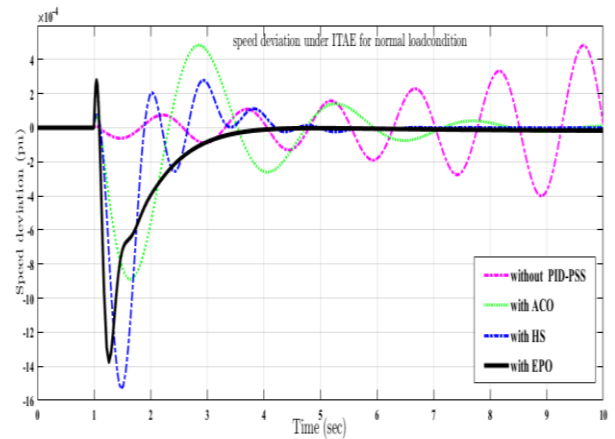


Fig 13 (b) Speed deviation for regular load

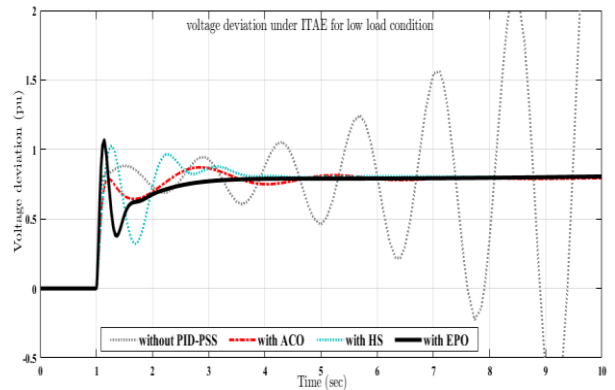


Fig 14 (a) Voltage deviation for luminous load

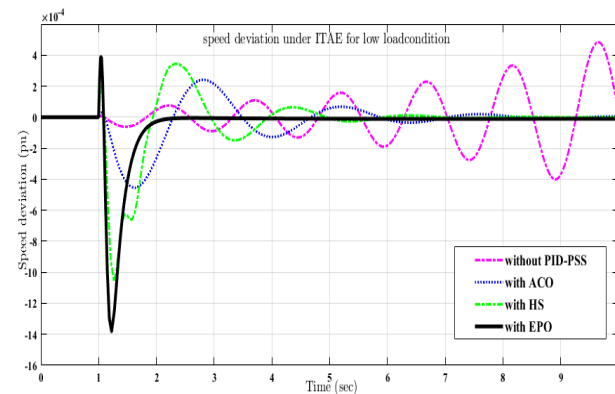


Fig 14 (b) Speed deviation for luminous load

Above shown figures 12, 13 and 14 are the responses under ITAE criteria for full, regular and luminous loading conditions respectively. Best fit value for ITAE criteria is 59.5631. Table 4 represents the tuned values of controller and table 5 represents overshoot time and settling time for voltage and speed deviation for different loading conditions.

Below section represents the tuned control parameters of FOPID-PSS and settling time and overshoot time for voltage and speed deviation.

Table 4 representation of FOPID-PSS parameters under ITAE criteria for different loads

| Operating condition | Tuning methods | Tuned controlled parameters | | | | | | | |
|---|-----------------|-----------------------------|--------|--------|-----------|--------|--------|--------|--------|
| | | P | I | D | λ | μ | Kpss | T1 | T2 |
| Case1 P=1.8, Q=1.0 (Full load) | Without PID-PSS | – | – | – | – | – | – | – | – |
| | ACO PID-PSS | 0.7395 | 0.5015 | 0.9498 | 0.2568 | 0.5698 | 0.7501 | 0.0196 | 0.7552 |
| | HS PID-PSS | 0.6436 | 0.3575 | 0.9934 | 0.5478 | 0.2335 | 0.6262 | 0.5389 | 0.5389 |
| | EPO PID-PSS | 0.6005 | 0.3133 | 0.8562 | 0.9891 | 0.4459 | 0.0787 | 0.3922 | 0.0012 |
| Case2 P=1.5, Q=0.8 (Regular load) | Without PID-PSS | – | – | – | – | – | – | – | – |
| | ACO PID-PSS | 4.7258 | 2.5647 | 0.0598 | 0.2239 | 0.9987 | 6.4062 | 2.0851 | 5.1564 |
| | HS PID-PSS | 4.1053 | 2.5387 | 0.0261 | 0.2856 | 0.5654 | 4.1173 | 1.0181 | 1.3198 |
| | EPO PID-PSS | 0.6804 | 0.6227 | 0.7895 | 0.3556 | 0.2110 | 0.9770 | 0.5037 | 0.5639 |
| Case3 P=0.7, Q=0.3 (Luminous load) | Without PID-PSS | – | – | – | – | – | – | – | – |
| | ACO PID-PSS | 4.7537 | 9.8511 | 0.5440 | 0.2997 | 0.5461 | 9.6564 | 3.6627 | 4.9476 |
| | HS PID-PSS | 0.9336 | 0.2773 | 0.0260 | 0.2354 | 0.8521 | 0.8235 | 0.9784 | 0.4603 |
| | EPO PID-PSS | 0.8166 | 0.0306 | 0.0674 | 0.6598 | 0.7784 | 0.7636 | 0.2147 | 0.0280 |

Table 5 Overshoot time and settling time for deviation in speed and terminal voltage under ITAE criteria

| Operating conditions | Tuning methods | Deviation in Terminal voltage | | Deviation in speed | |
|--|-----------------|-------------------------------|-------------------------|-----------------------|-------------------------|
| | | Overshoot time (pu) | Settling time (seconds) | Overshoot time (pu) | Settling time (seconds) |
| Case1 P=1.8, Q=1.0 (Full load) | Without PID-PSS | 0.80 | Inf | 0.10×10^{-4} | Inf |
| | ACO PID-PSS | 1.01 | 7.50 | 0.30×10^{-4} | 8.30 |
| | HS PID-PSS | 1.30 | 4.20 | 0.15×10^{-4} | 3.80 |
| | EPO PID-PSS | 1.01 | 2.22 | 3.10×10^{-4} | 2.50 |
| Case2 P=1.5, Q=0.8 (Regular load) | Without PID-PSS | 0.80 | Inf | 0.10×10^{-4} | Inf |
| | ACO PID-PSS | 1.10 | 4.80 | 1.01×10^{-4} | 8.20 |
| | HS PID-PSS | 1.02 | 3.90 | 1.20×10^{-4} | 5.50 |
| | EPO PID-PSS | 1.00 | 2.70 | 2.90×10^{-4} | 3.42 |
| Case3 P=0.7, Q=0.3 (Luminous load) | Without PID-PSS | 0.80 | Inf | 0.10×10^{-4} | Inf |
| | ACO PID-PSS | 0.82 | 6.80 | 0.10×10^{-4} | 8.01 |
| | HS PID-PSS | 0.65 | 4.00 | 2.10×10^{-4} | 7.10 |
| | EPO PID-PSS | 1.11 | 2.95 | 4.00×10^{-4} | 2.27 |

Table 4 represents the controller parameters for different loading conditions under ITAE criteria. Without controller no values are specified and then with the help of ACO, HS algorithm and EPO values are obtained by running these algorithms. Eagle Perching Optimization algorithm is considered

as best algorithm as it gives stable and desired values as compared to other algorithms. Table 5 represents the overshoot time (pu) and settling time (seconds) for voltage and speed deviation for different loads. Settling time with less value is considered as the best value.

8.2 Analysis on the basis of ISE criteria

Below figures represent the waveform for integral of square error. Waveform is represented firstly for full load, secondly for regular load and then for light loading conditions. Analysis is done on the basis of speed deviation and terminal voltage deviation.

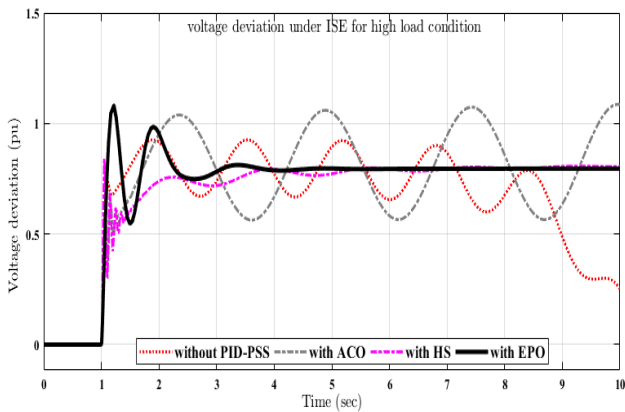


Fig 15 (a) Voltage deviation for full load

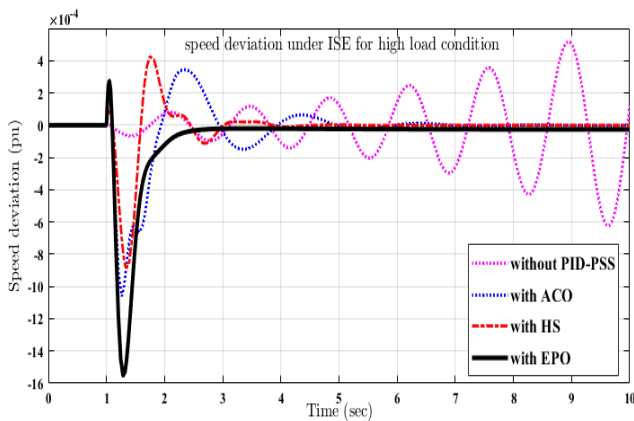


Fig 15 (b) Speed deviation for full load

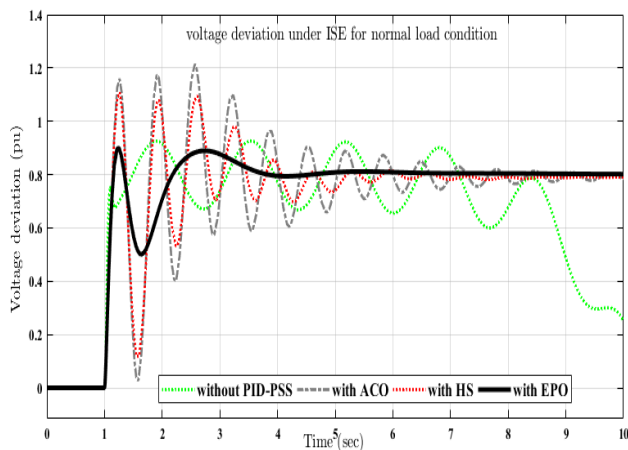


Fig 16 (a) Voltage deviation for regular load

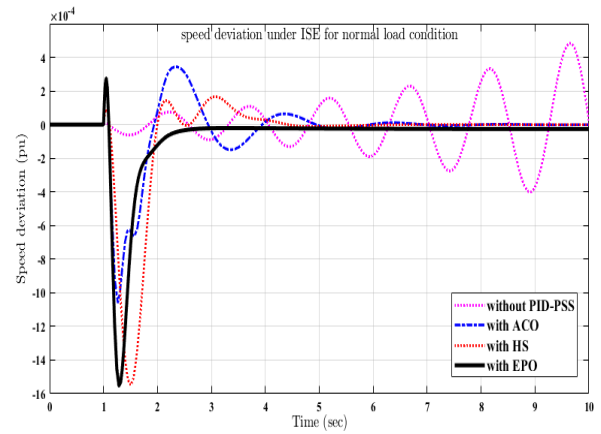


Fig 16 (b) Speed deviation for regular load

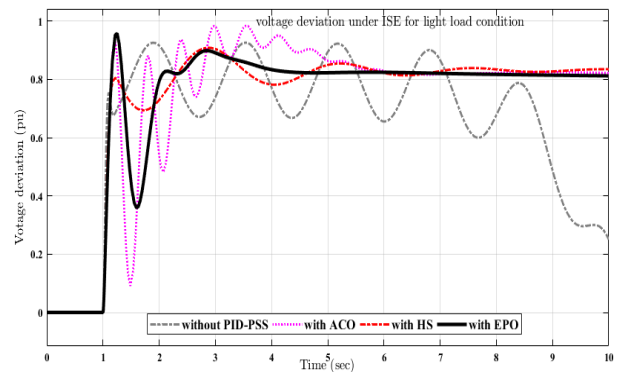


Fig 17 (a) Voltage deviation for luminous load

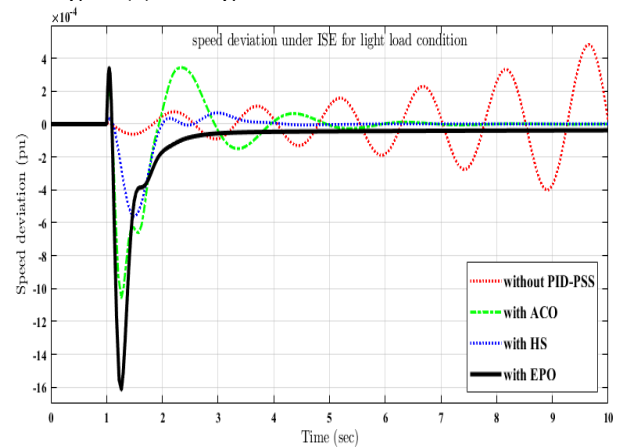


Fig 17 (b) Speed deviation for luminous load

Above shown figures 15, 16 and 17 are the responses under ISE criteria for full, regular and luminous loading conditions respectively. Best fit value for ISE criteria is 5.2663. All three figures specify the responses of voltage deviation (pu) and speed deviation (pu) in y-axis and time (sec) in x-axis. Table 6 represents the tuned values of controller and table 7 represents overshoot time and settling time for voltage and speed deviation for different loading conditions. Without PID-PSS there is no value of controller and by tuning the parameters values obtained are mentioned below in tables.

Table 6 representation of FOPID-PSS parameters under ISE criteria for different loads

| Operating condition | Tuning methods | Tuned controlled parameters | | | | | | | |
|---|-----------------|-----------------------------|--------|--------|-----------|--------|--------|--------|--------|
| | | P | I | D | λ | μ | Kpss | T1 | T2 |
| Case1 P=1.8, Q=1.0 (Full load) | Without PID-PSS | – | – | – | – | – | – | – | – |
| | ACO PID-PSS | 0.7921 | 0.8959 | 0.9857 | 0.5451 | 0.6659 | 0.9503 | 0.9250 | 0.8732 |
| | HS PID-PSS | 0.7156 | 0.6021 | 0.8117 | 0.2665 | 0.8594 | 0.8329 | 0.7662 | 0.4009 |
| | EPO PID-PSS | 0.5536 | 0.3520 | 0.0795 | 0.5214 | 0.6398 | 0.6126 | 0.5548 | 0.1504 |
| Case2 P=1.5, Q=0.8 (Regular load) | Without PID-PSS | – | – | – | – | – | – | – | – |
| | ACO PID-PSS | 3.9255 | 7.0167 | 0.3048 | 0.7714 | 0.6689 | 6.1315 | 9.0329 | 1.3488 |
| | HS PID-PSS | 0.9575 | 0.9649 | 0.2717 | 0.2232 | 0.4487 | 0.9757 | 0.9572 | 0.4854 |
| | EPO PID-PSS | 0.7935 | 0.6947 | 0.1576 | 0.3365 | 0.2035 | 0.9706 | 0.8011 | 0.0355 |
| Case3 P=0.7, Q=0.3 (Luminous load) | Without PID-PSS | – | – | – | – | – | – | – | – |
| | ACO PID-PSS | 4.1723 | 9.6753 | 0.8116 | 0.8547 | 0.9913 | 9.8512 | 1.6255 | 1.5176 |
| | HS PID-PSS | 2.9913 | 0.9058 | 0.0380 | 0.2015 | 0.6034 | 5.8507 | 0.8512 | 0.7293 |
| | EPO PID-PSS | 0.9626 | 0.0545 | 0.0375 | 0.2285 | 0.2014 | 0.6797 | 0.0965 | 0.0915 |

Table 7 overshoot time and settling time for deviation in speed and terminal voltage under ISE criteria

| Operating conditions | Tuning methods | Deviation in speed | | Deviation in Terminal voltage | |
|---|-----------------|---------------------|-------------------------|-------------------------------|-------------------------|
| | | Overshoot time (pu) | Settling time (seconds) | Overshoot time (pu) | Settling time (seconds) |
| Case1 P=1.8, Q=1.0 (Full load) | Without PID-PSS | 0.75 | Inf | 0.20×10^{-4} | Inf |
| | ACO PID-PSS | 0.62 | Inf | 0.98×10^{-4} | 5.01 |
| | HS PID-PSS | 0.80 | 5.55 | 0.83×10^{-4} | 4.00 |
| | EPO PID-PSS | 1.12 | 4.02 | 2.51×10^{-4} | 2.51 |
| Case2 P=1.5, Q=0.8 (Regular load) | Without PID-PSS | 0.75 | Inf | 0.20×10^{-4} | Inf |
| | ACO PID-PSS | 1.18 | 9.85 | 0.81×10^{-4} | 7.02 |
| | HS PID-PSS | 1.15 | 7.01 | 1.02×10^{-4} | 5.20 |
| | EPO PID-PSS | 0.85 | 4.12 | 2.90×10^{-4} | 2.81 |
| Case3 P=0.7, Q=0.3 (Luminous load) | Without PID-PSS | 0.75 | Inf | 0.20×10^{-4} | Inf |
| | ACO PID-PSS | 0.95 | 6.01 | 2.01×10^{-4} | 5.20 |
| | HS PID-PSS | 0.81 | 5.80 | 0.10×10^{-4} | 4.15 |
| | EPO PID-PSS | 0.98 | 4.73 | 2.80×10^{-4} | 2.72 |

Table 6 represents the controller parameters for different loading conditions under ISE criteria. Without controller no values are specified and then with the help of Ant Colony Optimization (ACO),

Harmony Search algorithm and Eagle Perching Optimization values are obtained by running these algorithms. Eagle Perching Optimization algorithm is considered as best algorithm as it gives stable

and desired values as compared to other algorithms. Table 7 represents the overshoot time (pu) and settling time (seconds) for voltage and speed deviation for different loads. Settling time with less value is considered as the best value.

Below section represents the analysis on the basis of integral of absolute error criteria generally known as IAE criteria. Different loading conditions are also analysed.

8.3 Analysis on the basis of IAE criteria

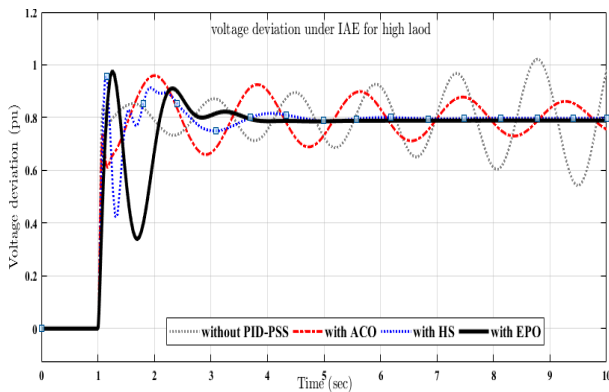


Fig 18 (a) Voltage deviation for full load

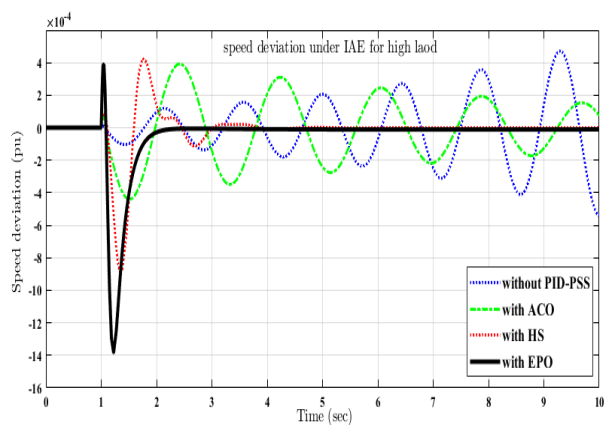


Fig 18 (b) Speed deviation for full load

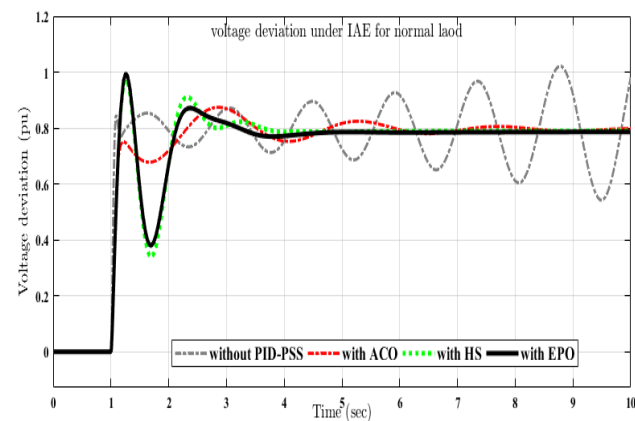


Fig 19 (a) Voltage deviation for regular load

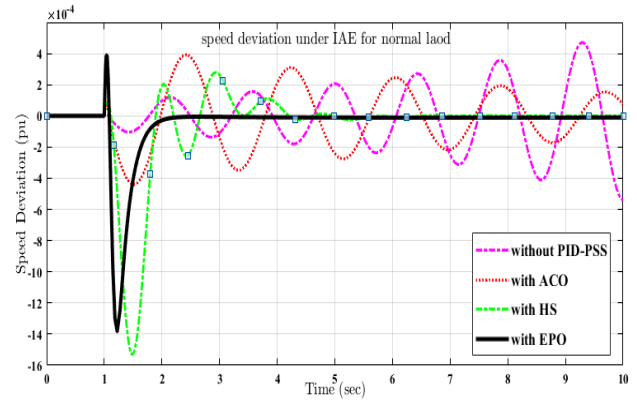


Fig 19 (b) Speed deviation for regular load

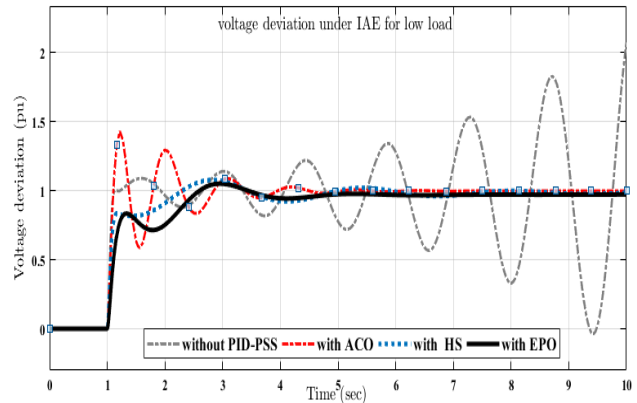


Fig 20 (a) Voltage deviation for regular load

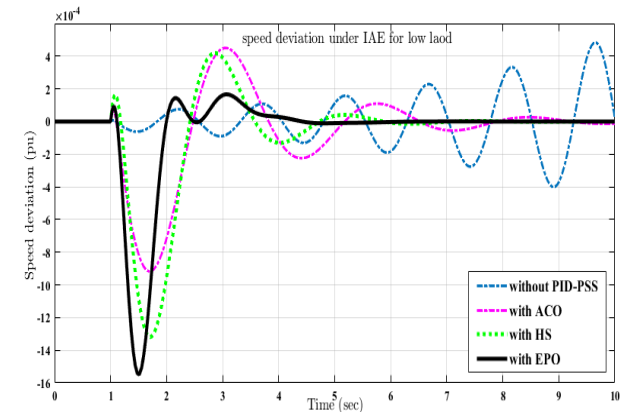


Fig 20 (b) Speed deviation for regular load

Above shown figures 18, 19 and 20 are the responses under IAE criteria for full, regular and luminous loading conditions respectively. Best fit value for IAE criteria is 1.8643. All three figures specify the responses of voltage deviation (pu) and speed deviation (pu) in y-axis and time (sec) in x-axis. Table 8 represents the tuned values of controller and table 9 represents overshoot time and settling time for voltage and speed deviation for different loading conditions. Without PID-PSS there is no value of controller and by tuning the parameters values obtained are mentioned below in tables

Table 8 Representation of FOPID-PSS parameters under IAE criteria for different loads

| Operating condition | Tuning methods | Tuned controlled parameters | | | | | | | |
|---|-----------------|-----------------------------|--------|--------|-----------|--------|--------|--------|--------|
| | | P | I | D | λ | μ | Kpss | T1 | T2 |
| Case1 P=1.8, Q=1.0 (Full load) | Without PID-PSS | – | – | – | – | – | – | – | – |
| | ACO PID-PSS | 0.7771 | 0.7867 | 0.6421 | 0.5532 | 0.4296 | 0.8038 | 0.9460 | 0.5341 |
| | HS PID-PSS | 0.5009 | 0.5386 | 0.6228 | 0.2251 | 0.6987 | 0.6366 | 0.4582 | 0.3198 |
| | EPO PID-PSS | 0.4717 | 0.1664 | 0.5435 | 0.2056 | 0.6059 | 0.5713 | 0.3338 | 0.2901 |
| Case2 P=1.5, Q=0.8 (Regular load) | Without PID-PSS | – | – | – | – | – | – | – | – |
| | ACO PID-PSS | 2.9324 | 0.4226 | 0.7876 | 0.8184 | 0.7854 | 0.9854 | 0.8554 | 1.7045 |
| | HS PID-PSS | 1.1440 | 0.4126 | 0.0565 | 0.3652 | 0.5421 | 0.7124 | 0.5615 | 1.0581 |
| | EPO PID-PSS | 0.2330 | 0.3068 | 0.0268 | 0.7896 | 0.6547 | 0.3926 | 0.6636 | 0.1220 |
| Case3 P=0.7, Q=0.3 (Luminous load) | Without PID-PSS | – | – | – | – | – | – | – | – |
| | ACO PID-PSS | 4.2252 | 9.4985 | 0.0265 | 0.2259 | 0.2270 | 7.9399 | 1.0181 | 5.0764 |
| | HS PID-PSS | 2.7236 | 0.1538 | 0.0165 | 0.6380 | 0.7899 | 5.5631 | 1.0551 | 1.3198 |
| | EPO PID-PSS | 0.9800 | 0.0215 | 0.0039 | 0.9971 | 0.5254 | 0.9232 | 0.3000 | 0.1287 |

Table 9 overshoot time and settling time for deviation in speed and terminal voltage under IAE criteria

| Operating conditions | Tuning methods | Deviation in speed | | Deviation in Terminal voltage | |
|--|-----------------|---------------------|-------------------------|-------------------------------|-------------------------|
| | | Overshoot time (pu) | Settling time (seconds) | Overshoot time (pu) | Settling time (seconds) |
| Case1 P=1.8, Q=1.0 (Full load) | Without PID-PSS | 0.82 | Inf | 0.10×10^{-4} | Inf |
| | ACO PID-PSS | 0.72 | Inf | 2.01×10^{-4} | Inf |
| | HS PID-PSS | 0.83 | 4.80 | 2.23×10^{-4} | 3.98 |
| | EPO PID-PSS | 0.98 | 3.62 | 4.00×10^{-4} | 2.12 |
| Case2 P=1.5, Q=0.8 (Regular load) | Without PID-PSS | 0.82 | Inf | 0.10×10^{-4} | Inf |
| | ACO PID-PSS | 0.78 | 8.50 | 0.15×10^{-4} | Inf |
| | HS PID-PSS | 0.97 | 4.70 | 2.05×10^{-4} | 5.55 |
| | EPO PID-PSS | 1.00 | 3.35 | 4.01×10^{-4} | 2.27 |
| Case3 P=0.7, Q=0.3 (Luminous load) | Without PID-PSS | 0.82 | Inf | 0.10×10^{-4} | Inf |
| | ACO PID-PSS | 1.40 | 6.12 | 0.70×10^{-4} | 9.01 |
| | HS PID-PSS | 0.85 | 5.54 | 1.82×10^{-4} | 6.45 |
| | EPO PID-PSS | 0.83 | 4.81 | 0.90×10^{-4} | 4.80 |

Table 8 represents the controller parameters for different loading conditions under IAE criteria. Eagle Perching Optimization algorithm is considered as best algorithm as it gives stable Table 9 represents the overshoot time (pu) and settling time (seconds) for voltage and speed

deviation for different loads. Settling time with less value is considered as the best value.

Below section represents the brief conclusion of overall paper. Convergence characteristics are also shown in a comparative basis.

9 CONCLUSIONS

It is inferred from the above analyses that the FOPID-PSS designed by EPO provides better results relative to other algorithms. As it is shown that the system is initially undergoing oscillations at low frequencies. As a monitoring unit, PID-PSS is used to reduce oscillations.. Optimal PSS values are compatible with optimization strategies. Although the convergence rate of the EPO is much higher than that of ACO and HS. That is the basic aim of using multiple algorithms for optimization.

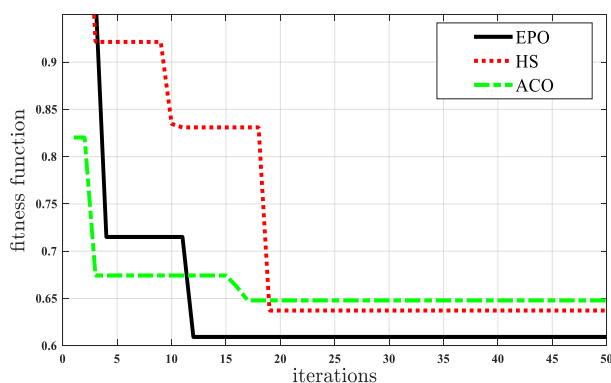


Fig 21. Convergence characteristics

Figure 21 represents the convergence characteristics of FOPID-PSS based synchronous machine system. Eagle Perching Optimization converges fast as compared to Ant colony Optimization and Harmony Search algorithm. From the convergence graph it is seen that EPO has very fast convergence rate that's why it is preferred as best optimization algorithm. In this paper every aspect is covered in context to single machine infinite bus (SMIB) system. Stability of SMIB system is compared according to three optimization techniques and three design criteria's and the hybrid controller is used to damp low frequency oscillations and disturbances occur in the system. To stabilize the parameters of the hybrid controller different optimization algorithms are used among which eagle perching optimization gives best and desired result.

References

[1] Al-Hinai, A. S., & Al-Hinai, S. M. (2009, January). Dynamic stability enhancement using particle swarm optimization power

system stabilizer. *In 2009 2nd International Conference on Adaptive Science & Technology (ICAST) (pp. 117-119). IEEE.*

- [2] Kasilingam, G. (2014). Particle swarm optimization based PID power system stabilizer for a synchronous machine. *World Academy of Science, Engineering and Technology, International Journal of Electrical, Computer, Energetic, Electronic and Communication Engineering*, 8(1), 111-116.
- [3] Jagadeesh, P., & Veeraj, M. S. (2016, February). Particle swarm optimization based power system stabilizer for SMIB system. *In 2016 International Conference on Emerging Trends in Engineering, Technology and Science (ICETETS) (pp. 1-6). IEEE.*
- [4] Abdul-ghaffar, H. I., Ebrahim, E. A., & Azzam, M. (2014). Design of PID controller for power system stabilization using ant colony optimization technique. *MEPCON'14, Cairo*.
- [5] Singh, M., Neema, D. D., & Patel, R. N. (2017). Improving Stability in Hydel Power System Using Ant Colony Optimized Tuned Controller. *i-Manager's Journal on Electrical Engineering*, 11(2), 16.
- [6] Hameed, K. A., & Palani, S. (2014). Robust design of power system stabilizer using harmony search algorithm. *automatika*, 55(2), 162-169.
- [7] Khan, A. T., Senior, S. L., Stanimirovic, P. S., & Zhang, Y. (2018). Model-free optimization using eagle perching optimizer. *arXiv preprint arXiv:1807.02754*.
- [8] Singh, M., Patel, R. N., & Neema, D. D. (2019). Robust tuning of excitation controller for stability enhancement using multi-objective metaheuristic Firefly algorithm. *Swarm and evolutionary computation*, 44, 136-147.
- [9] Singh, M., Patel, R. N., & Jhapt, R. (2016, January). Performance comparison of optimized controller tuning techniques for voltage stability. *In 2016 IEEE First International Conference on Control, Measurement and Instrumentation (CMI) (pp. 11-15). IEEE.*
- [10] Chaib, L., Choucha, A., & Arif, S. (2017). Optimal design and tuning of novel fractional order PID power system stabilizer using a new metaheuristic Bat algorithm. *Ain Shams Engineering Journal*, 8(2), 113-125.

- [11] Morsali, J., Kazemzadeh, R., & Azizian, M. R. (2015, May). Introducing FOPID-PSS to increase small-signal stability of multi-machine power system. In *2015 23rd Iranian Conference on Electrical Engineering* (pp. 1510-1515). IEEE.
- [12] Maurya, A. K., Bongulwar, M. R., & Patre, B. M. (2015, December). Tuning of fractional order PID controller for higher order process based on ITAE minimization. In *2015 Annual IEEE India Conference (INDICON)* (pp. 1-5). IEEE.
- [13] Soni, Y. K., & Bhatt, R. (2013). BF-PSO optimized PID controller design using ISE, IAE, IATE and MSE error criteria. *International Journal of Advanced Research in Computer Engineering & Technology (IJARCET)*, 2(7), 2333-2336.
- [14] Marzaki, M. H., Tajjudin, M., Rahiman, M. H. F., & Adnan, R. (2015, May). Performance of FOPI with error filter based on controllers performance criterion (ISE, IAE and ITAE). In *2015 10th Asian Control Conference (ASCC)* (pp. 1-6). IEEE.